EXPERIMENTAL ANALYSIS ON MELTING HEAT TRANSFER CHARACTERISTICS OF N-EICOSANE PCM IN A RECTANGULAR SYSTEM

Lucas Fernandes de Lima Lira, lucas.lira@ifb.edu.br
Antônio Brasil Junior, brasiljr@unb.br
Universidade de Brasília (UnB), Campus Universitário Darcy Ribeiro, Brasília, 70910-900, Brazil

Abstract. *The Latent thermal energy storage role in building demand control is gaining popularity as intermittent energy sources, such as solar photovoltaic or wind turbines, become more popular. In order to succeed, new suitable phase change materials (PCM) need to be identified. This paper presents an effort to develop a set of methodologies and common equipment to visualize melt front evolution during solid–liquid phase change process of materials to be used as energy store for heating or cooling applications. The methodology is applied to an n-eicosane PCM in a rectangular one side heated system. An Arduino board, combined with an HD webcam and a regular computer are used to control the entire system, record temperature profiles and capture melt front evolution. This data is then post processed in order to calculate melt fractions and heat transfer characteristics, including Nusselt and Rayleigh number on the hot wall. Results indicate that the methodology and equipment developed are efficient at inferring heat transfer mechanisms inside the system, including the dominant heat transfer mode and energy distribution at each time step, showing similar results as obtained by other researchers utilizing more complex, expensive and not portable equipment.*
Keywords*: Phase Change Material, Melting Heat Transfer, Thermal Storage*

1. NOMENCLATURE

NP	Number of pixels
$Q_{sens.}$	Absorbed sensible heat (kJ)
Q_{latent}	Absorbed latent heat (kJ)
Q_{Total}	Total absorbed heat (kJ)
cs	Specific heat (kJ/kgK)
h_{sl}	Latent heat (kJ/kg)
g	Acceleration of gravity (m2/s)
T	Temperature (K)
t	Time (s)
V	Volume (m3)
h	Heat transfer coefficient (W/m2K)
Nu	Nusselt number
SteFo	SteFo number
L	Length (m)
H	Height (m)
k	Thermal conductivity (W/mK)

Greek Symbols

ρ	Density (kg/m3)
α	Thermal diffusivity (m2/s)
β	Thermal expansion coeficient
γ	Melt fraction

Subscripts

l	Material at liquid state
s	Material at solid state
aver	Average value across volume
wall	Value over the heat plate
melting	Value referring to the PCM
.	melting point
i	time step

2. INTRODUCTION

The challenge of synchronizing demand and generation has become particularly relevant with the rise of renewable energy participation over the energy matrix (Cao, 2013) (Koukson, 2014) (Lira, 2012). In this setup, the use of phase change materials (PCM) in energy storage applications has gained importance. Storing thermal energy as latent heat allows large amounts of energy to be stored in relatively small volumes. The understanding of each system heat transfer characteristics is therefore essential.

The scarcity of studies regarding PCMs for residential cooling load control points towards the importance of developing methods and tools to analyse this kind of material (Yuan, 2014) (Sharma, 2009). Researches dedicated to the analysis of PCMs with melting point around 30ºC often require apparatus that, although are able to give a fair amount of information regarding the phase change process, require nontrivial equipment (such as PID controllers and dedicated system coolant) (Kamkari, 2013 and 2014) (Dhaidan, 2013) (Stritih,2004). This study introduces a methodology developed for the analysis of PCMs that may be used in building cooling demand control and, therefore, present melting

point below 40°C. The proposed model should be portable and of reduced cost, making it accessible to a wider range of researchers. The methodology will be applied to a n-eicosane paraffin, due to its record on heat transfer researches (Dhaidan, 2013) (Baby, 2015) (Brasil, 1985), and results compared against expectations.

3. EXPERIMENTAL APPARATUS AND PROCEDURE

The following sections describe the experimental apparatus designed for PCM analysis. It should be noted that its development aims to facilitate the access of researchers to this kind of study, reducing costs and increasing its portability. The built system can be divided into three main structures: A PCM enclosure, a heat exchanger and a control system.

3.1 PCM enclosure

The PCM container is formed by a 20mm thick acrylic frame over where five thin holes (1mm diameter) were drilled, allowing the insertion of thermocouples to measure the temperature across the PCM. This structure was mounted over a 20mm thick acrylic plate, forming an enclosure in which the PCM may be inserted. Details can be seen in the pictures below.

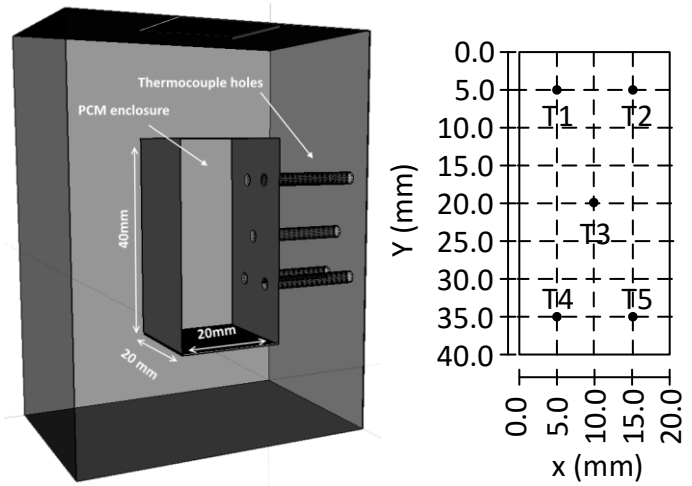

Figure 1 – PCM enclosure and thermocouples positioning (frontal view)

3.2 The heat exchanger system

A second structure was used to seal and heat the system. It consists on an acrylic ring with an internal gap of 30mm x 45mm where the heat exchanger, a 5 mm thick aluminum plate, was inserted. In order to measure the plate temperature, a small hole was drilled in one of its sidewalls and a thermocouple inserted.

Furthermore, three electrical resistances were combined in series and placed over the aluminum plate. An Arduino circuit was used to control the voltage across this circuit and, therefore, the plate temperature. To minimize losses, a 10 mm thick polystyrene block of was installed within the gap formed by the acrylic ring and the aluminum plate as illustrated at Figure 2. When superimposed, the storage structure and the heat exchanger structure form a closed system that seals the PCM enclosure and allows its heating and monitoring, as shown below.

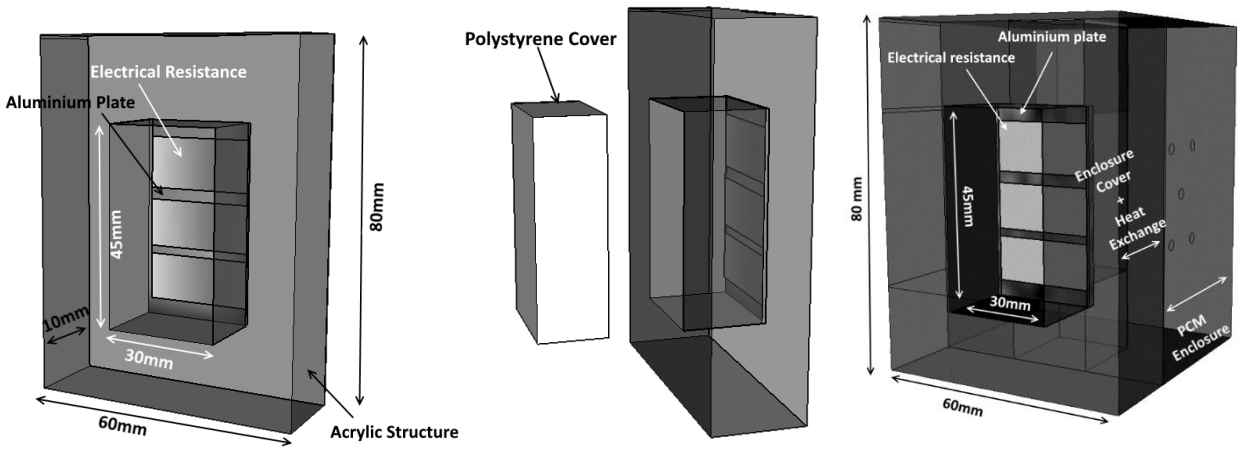

Figure 2 – View of the acrylic ring and aluminium plate, polystyrene insulation

3.3 PCM temperature control system

To measure and control the temperature throughout the system, the thermocouples described above were connected to an electronic circuit that combines an Arduino controller and integrated circuits (IC). The control algorithm reads the temperature of the thermocouple installed inside the aluminum plate and whenever it is below a given value, closes a relay, switching the heating system on. Once a set temperature is reached, the relay is opened, stopping any electrical current flowing through the resistors. To avoid cycling issues, it was allowed a hysteresis of 0.5°C around the target temperature.

Additionally, the temperature readings from the PCM and plate thermocouples are transmitted to a computer connected to the Arduino board and recorded at the time step of 30s.

3.4 Melting front monitoring system

In order to record the PCM melting front, a system containing an HD camera and a computer was set up. This system is also communicating with the Arduino circuit. The camera was placed at a distance of 15 cm from the compartment containing PCM, parallel to the plane to be documented. At every minute, a picture was taken and stored. Figure 3 is a simple schematic of the whole system combined.

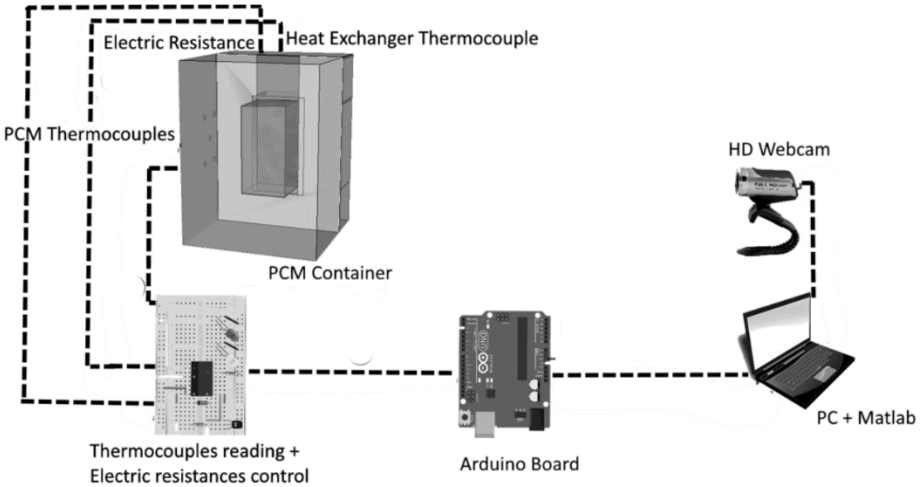

Figure 3 – System setup

3.5 Camera calibration

Matlab´s camera calibration toolbox was utilized to improve and evaluate the accuracy of the images captured by the camera. A series of pictures were taken with checkerboards positioned at the same plane as the PCM enclosure. These images were post processed, estimating the mean projection error of the camera. After calibration, it was found that the mean camera reprojection error is 0.31 pixels. This value will be used to estimate the uncertainties of the measured parameters (section 5).

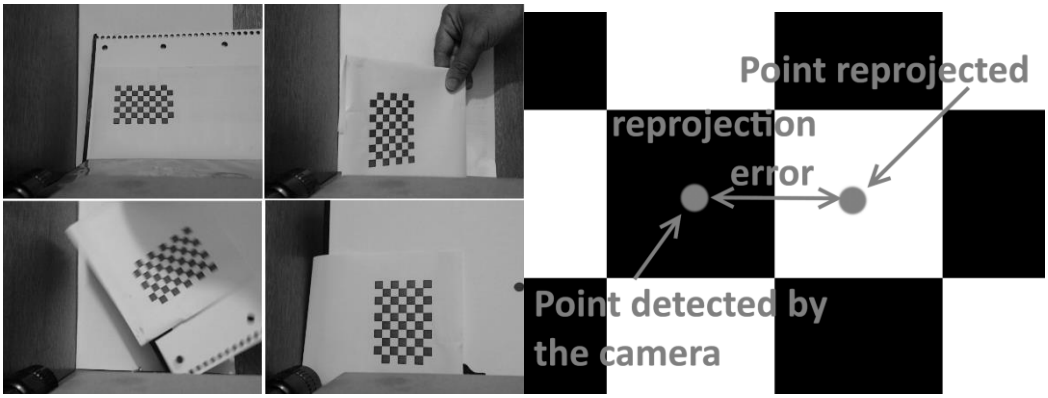

Figure 4 – Reprojection error analysis

3.6 PCM enclosure setup

The system setup started by melting the solid PCM in a water bath and then slowly adding it into the PCM reservoir, one layer at a time. Waiting one layer to solidify before adding a new one prevented the formation of air bubbles within the studied material. After sealing the system, the PCM reservoir was placed in front of the camera and the heating plate set to 2° C below the n-eicosane melting point. Once all the thermocouples inside the PCM read 34° C, the plate temperature was set to the new target and the system monitored as previously described at sections 2.5 and 2.6.

3– DATA ANALYSIS METHODOLOGY

3.1 Melt material

An important information to be gathered is the rate at which the PCM material melts.

For such, the pictures taken during the melt process were used as follows. First MATLAB image processing tool removed from these images anything but the PCM area. Next, the picture contrast was raised, followed by a threshold filtering which converted each original image into binary values. At this moment, any liquid PCM was represented by white pixels while solid l was shown as black pixels (Figure 5).

The percentage of solid material at any moment in the experiment was calculated using the formula below.

$$\gamma = \frac{NP_b}{NP_p} \qquad (1)$$

Where NPb represents the amount of black pixels in each image and NPP the total of pixels in the image.

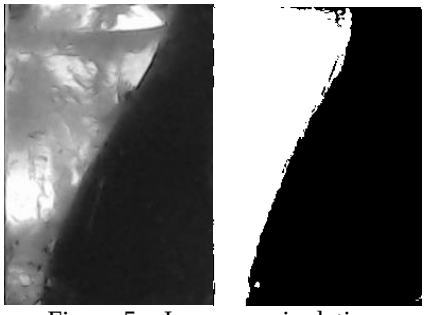

Figure 5 – Image manipulation

3.4 Melting rate

As the PCM starts the experiments at 2°C below its melting point, it is expected that the amount of sensible heat absorbed during the process is negligible when compared with the latent heat. If that is the case, the total absorbed energy can be estimated through the system melting rate, as follows.

$$Q_{total} = \frac{h_{sl} * dm}{dt} \quad (2)$$

Where,

$$\frac{dm}{dt} = \rho * (\gamma_i - \gamma_{i-1}) * V \quad (3)$$

Q_{total} represents the total absorbed energy at dt, ρ the PCM density and V the system volume.

3.5 Heat transfer coefficient

Once the total heat was calculated, the following formula was applied to estimate the heat transfer coefficient.

$$h(t) = \frac{Q(t)_{total}}{A_{wall}(T_{wall} - T_{aver})} \quad (4)$$

3.6 Dimensionless Parameters

Dimensionless parameters were defined as follows.

3.2.1 Nusselt Number

$$Nu(t) = \frac{h(t) * H}{k_l} \quad (5)$$

3.2.2 SteFo Number

$$Ste = \frac{c_p(T_{wall} - T_{melting})}{L} \quad (6)$$

$$Fo = \frac{\alpha t}{H^2} = \frac{kt}{c_p \rho H^2} \quad (7)$$

$$SteFo = Ste * Fo \quad (8)$$

3.2.3 Rayleigh Number

$$Ra = \frac{g\beta(T_w - T_f)H^3}{\nu\alpha} \quad (9)$$

4 MELT FRONT ANALYSIS – N-EICOSANE

4.1 - Hot wall at 50ºC

The methodology previously described was applied to the n-eicosane paraffin (C20H42) with the hot wall (aluminium plate) set to 50ºC .

Table 1 – n-eicosane properties [11]

Formula	*C20H42*
Melting temperature	36.4 ºC
Latent heat (hsl)	247.3 kJ/kg
Density (solid)	815 kg/m3
Density (liquid)	780 kg/m3
Liquid viscosity	$3.9*10^{-3}$ N-s/m^2
Specific heat (solid)	1.92 kJ/kgK
Specific heat (liquid)	2.46 kJ/kgK
Thermal expansion coefficient	$8.5*10^{-4}$ 1/K
Thermal Conductivity	0.158 W/mK

At first, it can be noted that the melt front is parallel to the hot wall, which indicates strong influence of heat conduction in the heat transfer process. This remains for as long as viscous force counterbalances the fluid movement. As this front becomes larger in volume, the development of buoyance force surpasses the viscous force, creating a circulating current within the PCM enclosure and the concave front form seen after 27 minutes of experiment (Figure 6). Figure 7 shows that at this same moment, the heat transfer coefficient behaviour changes from oscillating around a constant value to a small rise.

As the volume of liquid PCM within the enclosure rises, convection becomes more significant, increasing the curvature of the melt front and slightly raising the heat transfer coefficient. This trend is maintained until the melt front reaches the wall opposed to the hot wall. At that moment, the interface between solid and liquid material starts to reduce, which combined with an increase of internal temperatures, maintains the reducing heat transfer coefficient trend.

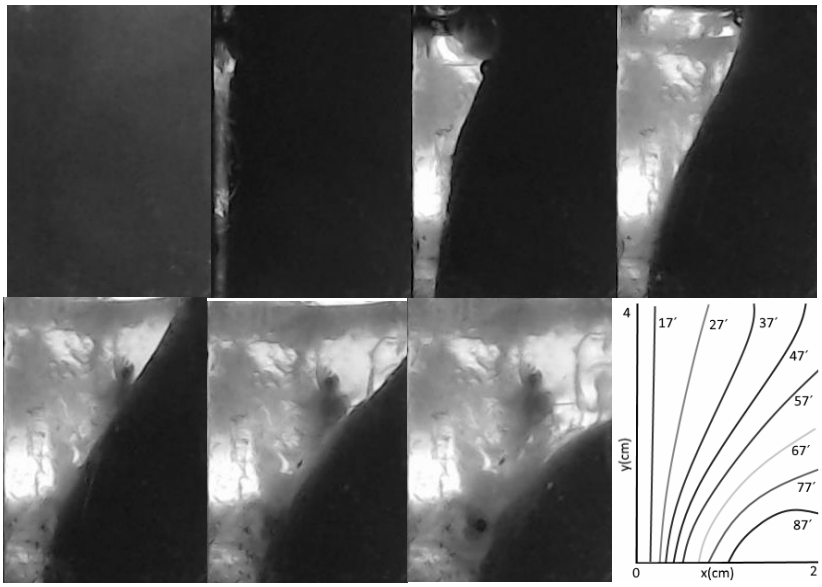

Figure 6 – melt front with hot wall at 50°C

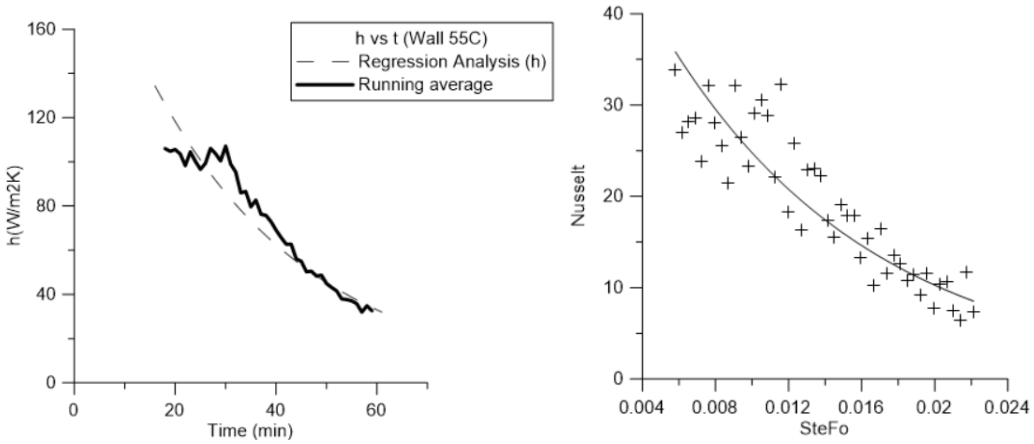

Figure 7 – Heat transfer coefficient vs time and Nusselt vs SteFo

4.2 – Hot wall at 65 oC

The same experiment was repeated with the hot wall temperature set to 65°C.

As expected, with a 65ºC hot wall (Ra=5x104), the heat transfer coefficient raised significantly, with the same amount of energy being transferred three times faster than it was observed with the previous hot wall setup.

Unfortunately, at this melting rate, the utilized equipment and procedure resulted into inconsistent data at the early stages of the experiment (period of conduction driven heat transfer). Once convection started, the gathered data could once again be used and resulted into consistent information. This indicates that there is a melting rate limit over where this methodology can be applied. Nevertheless, this should not be a problem when analysing materials for cooling load shifting as the hot wall temperature should be closer to the material melting point, and not 80% above it, as it is the case.

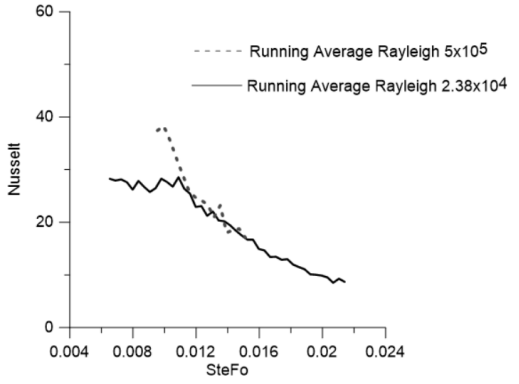

Figure 8 Nusselt vs SteFo

5- RESULTS RELIABILITY

Comparing the results with similar experiments performed by Kamkari indicates that the system performs as expected. The use of five thermocouples did not prove enough to generate an useful temperature profile within the PCM storage but was suitable to set the experiment initial conditions and to calculate the amount of latent and sensible heat absorbed at each time step.

The uncertainties of the measured results are dependent of the uncertainties associated to each measurement method. Moffat (1988) show that uncertainties in a result can be estimated using a root sum square combination of the uncertainty of each of the individual inputs. For example, given R(X1,X2,…,Xn), the uncertainty may be estimated as:

$$\delta R = \sqrt{\sum_{i=1}^{n} \left(\frac{\partial R}{\partial X_i} * \delta X_i \right)^2} \qquad (10)$$

Utilizing this method, it was found an 3.8% uncertainty for the absorbed energy, 8.1% regarding the heat transfer coefficient and 16.3% the Nusselt number. These values proved be almost unresponsive regarding the camera´s reprojection error, unlike to any uncertainty associated to thermocouple temperature and system dimensions.

6- CONCLUSION

The Arduino controlled system and developed analysis methodology were capable of characterizing the n-eicosane heat transfer on a rectangular enclosure with one heated surface. Two main cycles (a conduction driven and a convection driven period) were identified throughout the experiment both through visual inspection of the melt front and through the analysis of the heat transfer coefficient. The number of thermocouples utilized did not provide a useful profile of temperatures within the enclosure during the experiment, but was important to grant constant initial conditions during the several runs. Once the hot wall temperature was set to 80% of the n-eicosane melting point, the conduction driven period could not be characterised due the fast change over system conditions, indicating a limit to where the equipment may be applied. Uncertainties of 3.8% for the absorbed energy quantification, 8.1% for heat transfer coefficient and 16.3% for the Nusselt number are directly related to the thermocouple limitations. More accurate equipment could significantly reduce these values.

7- REFERENCES

Cao, S., Hasan, A., Siren, K., "On site energy matching indices for buildings with energy conversion, storage and hybrid grid connections". *Energy and Buildings*, vol.64, pp. 423-438, 2013.

Koukson, T., Bruel, P., Jamil., A. "Energy storage: Applications and challenges". Solar Energy Storage and Solar cells, vol. 120, pp. 59-80, 2014.

Lira, L., "Improving the operation of hybrid systems using detailed simulation". MPhil Dissertation. Dept. Mech. Eng. Strathclyde, UK.

Yuan, Y., Zhang, N., Tao, W., "Fatty acids as phase change materials: A review". Renewable and Sustainable Energy Reviews, vol. 29, pp. 482-498, 2014.

Sharma, A., Tyagi, V.V., Shen, C.R. "Review on thermal energy storage with phase change materials and applications".. Renewable and Sustainable Energy Reviews , vol. 13, pp. 318–345, 2009.

Kamkari, B., Shokouhmand, H. "Experimental investigation on melting heat transfer characteristics of lauric acid in a rectangular thermal storage unit". *International Journal of Heat and Mass Transfer* , vol. 50, pp. 201-212, 2013.

Kamkari, B.,Shokouhmand. H., "Experimental investigation of the effect of inclination angle on convection-driven melting of phase change material in a rectangular enclosure". *International Journal of Heat and Mass Transfer*, pp. 186-200, 2014.

Dhaidan, N. S., Khodadadi, J. M. "Melting and convection of phase change materials in different shape containers: A review". *Renewable and Sustainable Energy Review*, vol. 43, pp. 449-477, 2013

Stritih, U. "An experimental study of enhanced heat transfer in rectangular PCM thermal storage". *International Journal of Heat and Mass Transfer*, vol. 47, pp. 2841-2847, 2004.

Dhaidan1, N. S., Khodadadi, J.M. "Melting and convection of phase change materials in different shape containers: A review". *Renewable and Sustainable Energy Reviews*, vol. 43. pp.449-477, 2015.

Baby, R., Balaji, C., "Experimental investigations on phase change material based finned heat sinks for electronic equipment cooling". *International Journal of Heat and Mass Transfer*. Vol.55, pp. 1642-1649, 2012.

Brasil, A. "Outward Melting from Vertical Cylinder with Natural Convection Effects". In proceedings of the American Society of Mechanical Engineers, Miami Beach, Florida. November, 1985.

Hale, D. V., Hoovers, M. J., O'nell, M. J. "Phase Change Materials Handbook" . NASA. 1971.

Moffat, R. J., "Describing the uncertainties in experimental results", *Experimental Thermal and Fluid Science*, pp.3-17, 1988.

8. RESPONSIBILITY NOTICE

The authors are the only responsible for the printed material included in this paper.